Direct observation of two-color pulse dynamics in passively synchronized Er and Yb mode-locked fiber lasers

Wei-Wei Hsiang,[1,*] Wei-Chih Chiao,[1] Chia-Yi Wu,[1] and Yinchieh Lai[2,3]

[1]*Department of Physics, Fu Jen Catholic University, Taipei 24205, Taiwan*
[2]*Department of Photonics, National Chiao-Tung University, Hsinchu 300, Taiwan*
[3]*Research Center for Applied Sciences, Academia Sinica, Taipei 115, Taiwan*
[*]*069179@mail.fju.edu.tw*

Abstract: We report direct experimental observation of interesting pulse synchronization dynamics in a cavity-combined Er and Yb mode-locked fiber lasers by measuring the relative position between the two-color pulses in the shared fiber section. The influence of the 1.03 μm pulse on the 1.56 μm single pulse as well as bound soliton pairs can be clearly identified as an effective phase modulation through the XPM effect with the walk-off effect taken into account. For the 1.56 μm single pulse under synchronization, the dependence of the relative position variation and the center wavelength shift on the cavity mismatch detuning is found analogous to the typical characteristics of FM mode-locked lasers with modulation frequency detuning. Moreover, depending on the cavity mismatch, the passively synchronized 1.56 μm bound soliton pairs are found to exhibit two different dynamical behaviors, i.e., phase-locked (in-phase) as well as non-phase-locked. The physical origins for these two kinds of bound soliton pairs are investigated experimentally by disclosing their locations with respective to the copropagating 1.03 μm pulse.

OCIS codes: (140.3510) Lasers, fiber; (140.4050) Mode-locked lasers; (060.5530) Pulse propagation and temporal solitons; (320.7100) Ultrafast measurements.

References and links

1. C. Fürst, A. Leitenstorfer, and A. Laubereau, "Mechanism for self-synchronization of femtosecond pulses in a two-color Ti:sapphire laser," IEEE J. Sel. Top. Quantum Electron. **2**(3), 473–479 (1996).
2. G. Andriukaitis, T. Balčiūnas, S. Ališauskas, A. Pugžlys, A. Baltuška, T. Popmintchev, M.-C. Chen, M. M. Murnane, and H. C. Kapteyn, "90 GW peak power few-cycle mid-infrared pulses from an optical parametric amplifier," Opt. Lett. **36**(15), 2755–2757 (2011).
3. O. Chalus, A. Thai, P. K. Bates, and J. Biegert, "Six-cycle mid-infrared source with 3.8 μJ at 100 kHz," Opt. Lett. **35**(19), 3204–3206 (2010).
4. R. Selm, M. Winterhalder, A. Zumbusch, G. Krauss, T. Hanke, A. Sell, and A. Leitenstorfer, "Ultrabroadband background-free coherent anti-Stokes Raman scattering microscopy based on a compact Er:fiber laser system," Opt. Lett. **35**(19), 3282–3284 (2010).
5. M. Zhi and A. V. Sokolov, "Broadband coherent light generation in a Raman-active crystal driven by two-color femtosecond laser pulses," Opt. Lett. **32**(15), 2251–2253 (2007).
6. R. Weigand, J. T. Mendonça, and H. M. Crespo, "Cascaded nondegenerate four-wave-mixing technique for high-power single-cycle pulse synthesis in the visible and ultraviolet ranges," Phys. Rev. A **79**(6), 063838 (2009).
7. A. Bartels, N. R. Newbury, I. Thomann, L. Hollberg, and S. A. Diddams, "Broadband phase-coherent optical frequency synthesis with actively linked Ti:sapphire and Cr:forsterite femtosecond lasers," Opt. Lett. **29**(4), 403–405 (2004).
8. D. Yoshitomi, X. Zhou, Y. Kobayashi, H. Takada, and K. Torizuka, "Long-term stable passive synchronization of 50 μJ femtosecond Yb-doped fiber chirped-pulse amplifier with a mode-locked Ti:sapphire laser," Opt. Express **18**(25), 26027–26036 (2010).
9. Z. Wei, Y. Kaboyashi, and K. Torizuka, "Passive synchronization between femtosecond Ti:sapphire and Cr:forsterite lasers," Appl. Phys. B **74**(9), S171–S176 (2002).
10. M. Rusu, R. Herda, and O. G. Okhotnikov, "Passively synchronized erbium (1550-nm) and ytterbium (1040-nm) mode-locked fiber lasers sharing a cavity," Opt. Lett. **29**(19), 2246–2248 (2004).
11. M. Rusu, R. Herda, and O. Okhotnikov, "Passively synchronized two-color mode-locked fiber system based on master-slave lasers geometry," Opt. Express **12**(20), 4719–4724 (2004).

#154459 - $15.00 USD Received 12 Sep 2011; revised 2 Nov 2011; accepted 3 Nov 2011; published 15 Nov 2011

12. W.-W. Hsiang, C.-H. Chang, C.-P. Cheng, and Y. Lai, "Passive synchronization between a self-similar pulse and a bound-soliton bunch in a two-color mode-locked fiber laser," Opt. Lett. **34**(13), 1967–1969 (2009).
13. W. Chang, N. Akhmediev, and S. Wabnitz, "Effect of external periodic potential on pairs of dissipative solitons," Phys. Rev. A **80**(1), 013815 (2009).
14. W. Chang, N. Akhmediev, S. Wabnitz, and M. Taki, "Influence of external phase and gain-loss modulation on bound solitons in laser systems," J. Opt. Soc. Am. B **26**(11), 2204–2210 (2009).
15. Y. J. He, B. A. Malomed, D. Mihalache, B. Liu, H. C. Huang, H. Yang, and H. Z. Wang, "Bound states of one-, two-, and three-dimensional solitons in complex Ginzburg-Landau equations with a linear potential," Opt. Lett. **34**(19), 2976–2978 (2009).
16. H. G. Winful and D. T. Walton, "Passive mode locking through nonlinear coupling in a dual-core fiber laser," Opt. Lett. **17**(23), 1688–1690 (1992).
17. J. Atai and B. A. Malomed, "Bound states of solitary pulses in linearly coupled Ginzburg-Landau equations," Phys. Lett. A **244**(6), 551–556 (1998).
18. H. E. Nistazakis, D. J. Frantzeskakis, J. Atai, B. A. Malomed, N. Efremidis, and K. Hizanidis, "Multichannel pulse dynamics in a stabilized Ginzburg-Landau system," Phys. Rev. E Stat. Nonlin. Soft Matter Phys. **65**(3 3 Pt 2B), 036605 (2002).
19. P. L. Baldeck, R. R. Alfano, and G. P. Agrawal, "Induced-frequency shift of copropagating ultrafast optical pulses," Appl. Phys. Lett. **52**(23), 1939–1941 (1988).
20. A. E. Siegman and D. J. Kuizenga, "Modulation frequency detuning effects in the FM Mode-locked laser," IEEE J. Quantum Electron. **6**(12), 803–808 (1970).
21. M. J. Lederer, B. Luther-Davies, H. H. Tan, C. Jagadish, N. N. Akhmediev, and J. M. Soto-Crespo, "Multipulse operation of a Ti:sapphire laser mode locked by an ion-implanted semiconductor saturable-absorber mirror," J. Opt. Soc. Am. B **16**(6), 895–904 (1999).
22. B. Ortaç, A. Zaviyalov, C. K. Nielsen, O. Egorov, R. Iliew, J. Limpert, F. Lederer, and A. Tünnermann, "Observation of soliton molecules with independently evolving phase in a mode-locked fiber laser," Opt. Lett. **35**(10), 1578–1580 (2010).

1. Introduction

The technique of passive synchronization based on the combined effects of cross phase modulation (XPM) and anomalous group velocity dispersion (GVD) [1] has been demonstrated to be an effective method to generate synchronized two-color ultrashort mode-locked pulse trains for many potential applications. These include the ultrafast optical parametric amplifier (OPA) [2, 3], coherent anti-Stokes Raman scattering (CARS) microscopy [4], and coherent optical pulse/frequency synthesis [5–7]. By utilizing the combined cavities or the master-slave configuration, the two-color pulses overlap and interact with each other in a laser crystal or fiber section such that the precise locking of pulse repetition rates between two mode-locked lasers with different wavelengths can be achieved. Although the passive synchronization technique mentioned above has been successfully used in a variety of ultrafast laser systems [1, 8–12], most of the studies focused on the timing jitter reduction between the two-color pulses and only a few works paid attention to study the underlying two-color pulse dynamics in the passive synchronization by analyzing the relationship between the laser center wavelength shift and the cavity mismatch [1, 9]. However, one of the most direct and important aspects in these experiments, i.e., the relative pulse position during copropagating, has not been investigated carefully so far. With the knowledge of the relative position as well as the individual pulse widths of the two-color pulses, how these pulses interact and affect each other during the passive synchronization process can be fully understood. This issue is also worthy of investigation for the more complicated case in which the 1.56 μm multiple-pulse bound states are synchronized with another copropagating 1.03 μm pulse in the two-color fiber lasers [12]. The observed dynamical behaviors of the 1.56 μm bound pulses under the influence of another copropagating pulse at 1.03 μm may be able to give new insights into the understanding of the general complex Ginzburg-Landau equation (CGLE) with an external potential [13–15] as well as the pulse interaction dynamics described by the coupled CGLEs [16–18].

In this paper, we report direct experimental observation results of two-color pulse dynamics under passive synchronization by measuring their relative pulse position in the shared fiber section of the cavity-combined Er and Yb mode-locked fiber lasers. A collinear sum-frequency generation (SFG) cross-correlator is built to perform the relative position measurement between the 1.56 μm and 1.03 μm pulses. It is found that the 1.56 μm fs pulses pass through a significant portion of the 1.03 μm chirped ps pulse and experience the

#154459 - $15.00 USD Received 12 Sep 2011; revised 2 Nov 2011; accepted 3 Nov 2011; published 15 Nov 2011

frequency shifts through the XPM effects to maintain the passive synchronization. By analyzing the dependence of the relative position on the cavity mismatch detuning, the effects of the cross-phase modulation, the pulse walk-off, the group velocity dispersion, and the laser center wavelength restoration on the two-color pulse dynamics under synchronization can be clearly identified. Moreover, depending on the cavity mismatch, the passively synchronized 1.56 μm bound soliton pairs are found to be able to exhibit two different dynamical behaviors. They can be either in-pahse phase-locked or not phase-locked at all. The origins of these two kinds of bound soliton pairs are investigated experimentally by disclosing their locations with respective to the copropagating 1.03 μm pulse.

2. Passively synchronized Er and Yb mode-locked fiber lasers

2.1 Experimental setup

The schematic of the cavity-combined Er and Yb mode-locked fiber lasers in our passive synchronization experiment is shown in Fig. 1(a). The setup of the two-color fiber lasers is similar to that in Ref [12], in which two polarization additive-pulse mode-locked (P-APM) Er-fiber and Yb-fiber lasers are combined by utilizing the two 1560/1030 nm wavelength division multiplexers (WDM3 and MDM4). The 1.56 μm and 1.03 μm pulses can interact through the XPM effect in the shared fiber section and accordingly adjust their pulse repetition rates to achieve the synchronization. To be able to directly observe the pulse dynamics of the synchronized two-color pulses, their original relative positions in the shared fiber section are needed to be known. For the purpose, two additional fiber couplers (C1 and C2) are added between WDM3 and WDM4 such that part of the copropagating two-color pulses without separation can be delivered directly into the cross-correlator for the relative position measurement. The output ratios of both fiber couplers C1 and C2 are 9% at 1.56 μm and 6% at 1.03 μm. In addition, compared to our previous experimental setup [12], the locations of the gain fibers are changed such that the amplified pulses in the Er-doped and Yb-doped fibers pass through the shared fiber section before they reach the polarization beam splitters. In this way enough pulse energies can be obtained from the couplers C1 and C2 for the followed cross-correlation trace measurements.

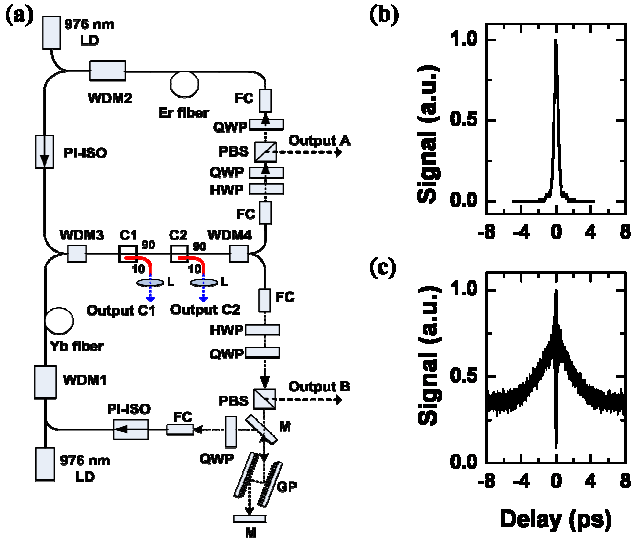

Fig. 1. (a) The schematic of the passively synchronized Er and Yb mode-locked fiber lasers. (b) and (c) The intensity and two-photon-absorption autocorrelation traces of the 1.56 μm and 1.03 μm respectively. WDM, wavelength division multiplexer (WDM1, 1030/976 nm; WDM2, 1560/976 nm; WDM3 and WDM4, 1560/1030 nm); LD, laser diode; PI-ISO, polarization-independent isolator; PBS, polarization beam splitter; FC, fiber collimator; GP, grating pair; QWP, quarter-wave plate; HWP, half-wave plate; C1 and C2, fiber couplers; M, mirror.

#154459 - $15.00 USD Received 12 Sep 2011; revised 2 Nov 2011; accepted 3 Nov 2011; published 15 Nov 2011

The passive synchronization can be achieved when the pulse repetition rates of the two individual mode-locked fiber lasers are close enough. In our setup the cavity length mismatch between the Er-fiber and Yb-fiber lasers can be tuned by moving one of the fiber collimators in the Yb-fiber laser. Besides, additional fine adjustments of the waveplates in the fiber lasers are also helpful to stabilize the synchronization. After stable passive synchronization is achieved, two stable pulse trains with the repetition rate of ~34.5 MHz are observed in the oscilloscope with the same trigger signal. Figure 1(b) and 1(c) shows the intensity autocorrelation trace of the 1.56 μm pulse and the two-photon absorption (TPA) interferometric autocorrelation trace of the 1.03 μm pulse. The corresponding FWHM pulse widths of the 1.56 μm and 1.03 μm pulses are 0.3 ps and 2.9 ps respectively. It indicates that in the shared fiber section the pulse width of the 1.03 μm pulse is much wider than that of the 1.56 μm pulse. These different pulse widths correspond to the distinct characteristics of stretched-pulse and self-similar mode-locking regimes. The net cavity group delay dispersion (GDD) of mode-locked Er-fiber and Yb-fiber lasers are estimated to be –0.03 ps^2 and 0.058 ps^2 respectively.

2.2 Relative position and walk-off of the two-color pulses in the shared fiber section

A home-built cross-correlator based on the collinear SFG configuration is utilized to measure their relative position, as shown in Fig. 2(a). By comparing the change of the relative positions measured simultaneously at the laser outputs C1 and C2 of Fig. 1(a), the two-color pulse walk-off during copropagation can be obtained as well. With the knowledge of the pulse walk-off, the relative position between the two-color pulses at any location in the shared fiber section can be evaluated from the results measured at the laser outputs C1 or C2. The fiber lengths of the output ports of both the couplers C1 and C2 are kept the same (~70 cm, the red lines in Fig. 1(a)).

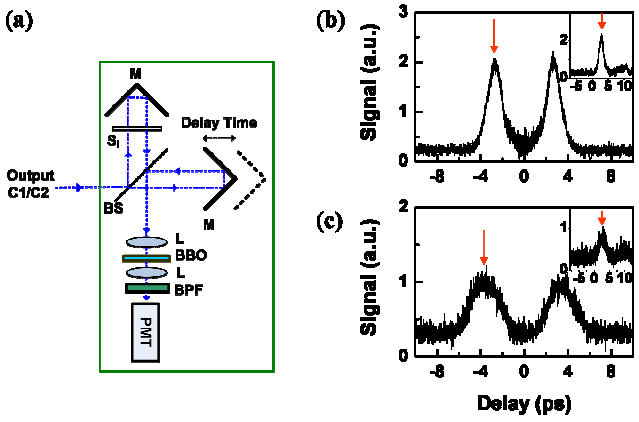

Fig. 2. (a) The setup of the cross-correlator. (b) and (c) The cross-correlation traces measured at the outputs C1 and C2 respectively (the thin Si filter removed). The insets show the measurement results when the thin Si filter is inserted. The red arrows indicate the intensity autocorrelation traces related to the third term in Eq. (2). PMT, photomultiplier tube; BPF, optical bandpass filter; BS, beam splitter; Si, thin Si filter; L, lens; M, mirror.

The home-built cross-correlator consists of a Michelson interferometer with the scanning delay, a BBO nonlinear crystal, an optical bandpass filter, and a photomultiplier tube (PMT). The incident light of the two-color pulses from the laser output is firstly split into two beams by the beam splitter (BS). After introducing the scanning delay in one arm of the interferometer, the two separated beams with and without the delay are combined on the beam splitter and then focused into a BBO crystal. The SFG signal after passing through the optical bandpass filter is detected by a photomultiplier tube (PMT) and can be expressed as

#154459 - $15.00 USD Received 12 Sep 2011; revised 2 Nov 2011; accepted 3 Nov 2011; published 15 Nov 2011

$$X_{SFG}(\tau) \propto \int_{-\infty}^{\infty} \left| E_{1.03}(t)E_{1.56}(t+\tau) + E_{1.03}(t+\tau)E_{1.56}(t) \right|^2 dt, \quad (1)$$

where τ is the scanning delay, and the electric fields of 1.56 μm and 1.03 μm pulses are represented by $E_{1.56}(t) = u_{1.56}(t)\exp(-i\omega_{1.56}t)$, $E_{1.03}(t) = u_{1.03}(t)\exp(-i\omega_{1.03}t)$, respectively. Equation (1) t

$$\begin{aligned} X_{SFG}(\tau) \propto & 2\int_{-\infty}^{\infty} I_{1.03}(t)I_{1.56}(t)dt + \int_{-\infty}^{\infty} I_{1.03}(t)I_{1.56}(t+\tau)dt + \int_{-\infty}^{\infty} I_{1.03}(t+\tau)I_{1.56}(t)dt \\ & + A(\tau)\cos(\omega_{1.03}\tau) + B(\tau)\cos(\omega_{1.56}\tau) + C(\tau)\cos[(\omega_{1.03}+\omega_{1.56})\tau] \\ & + D(\tau)\cos[(\omega_{1.03}-\omega_{1.56})\tau] \end{aligned} \quad , \quad (2)$$

where $I_{1.56}(t) = \left|u_{1.56}(t)\right|^2$, and $I_{1.03}(t) = \left|u_{1.03}(t)\right|^2$ are the intensities of 1.56 μm and 1.03 μm pulses. In Eq. (2), the first term represents the background dc SFG signal, the second and third terms are the two intensity cross-correlation traces corresponding to either the 1.56 μm or 1.03 μm pulses with the delay, and the last four terms are the rapidly oscillating ac SFG signals. The intensity cross-correlation traces can be extracted from $X_{SFG}(\tau)$ to identify the relative position. In the following, we illustrate how to identify the relative position as well as the pulse walk-off between the 1.56 μm and 1.03 μm pulses.

First of all, we measure the cross-correlation traces (the Si filter removed in Fig. 2(a)) at the laser outputs C1 and C2 simultaneously and the results are shown in Fig. 2(b) and 2(c) respectively. It can be clearly seen that in this case the sum of the rapidly oscillating ac SFG signals vanishes so that only the two intensity cross-correlation traces with the background dc SHG signal are remained. Therefore the time separation between the two-color pulses is just the absolute value of the delays for the peaks of the SFG signals, i.e., 2.7 ps in Fig. 2(b) and 3.8 ps in Fig. 2(c). Secondly, besides the separation of the two-color pulses, we need to determine which one of the two-color pulses leads the other. This can be simply achieved by inserting a thin Si filter in one arm of the interferometer to block the 1.03 μm pulses, as shown in Fig. 2(a). This results, on the one hand, the original second term $\int_{-\infty}^{\infty} I_{1.03}(t)I_{1.56}(t+\tau)dt$ in Eq. (2) to be diminished. On the other hand, the original third term $\int_{-\infty}^{\infty} I_{1.03}(t+\tau)I_{1.56}(t)dt$ in Eq. (2) will turn to $\int_{-\infty}^{\infty} I_{1.03}(t+\tau)I_{1.56}(t+\tau_{Si})dt$, where τ_{Si} is the additional delay introduced by the thin Si filter. The peaks, indicated by the red arrows in Fig. 2(b) and its inset, correspond to the intensity cross-correlation traces of $\int_{-\infty}^{\infty} I_{1.03}(t+\tau)I_{1.56}(t)dt$ and $\int_{-\infty}^{\infty} I_{1.03}(t+\tau)I_{1.56}(t+\tau_{Si})dt$ respectively. Therefore the peak of $\int_{-\infty}^{\infty} I_{1.03}(t+\tau)I_{1.56}(t)dt$ located at a negative delay of −2.7 ps in Fig. 2(b) indicates that the 1.56 μm pulse leads the 1.03 μm pulse at the laser output C1. Similarly, Fig. 2(c) and its inset show that the 1.56 μm pulse leads the 1.03 μm pulse by 3.8 ps at the output C2. By comparing the relative position variation between the outputs C1 and C2 one can conclude that the group velocity mismatch $(\frac{1}{v_{g,1.56}} - \frac{1}{v_{g,1.03}})$ between the 1.56 μm and 1.03 μm pulses in the two fiber couplers (65-cm-long HI 1060 fiber) is ~-1.7 ps/m.

In addition, we have also measured the pulse walk-off in the WDM3 and WDM4, which is comprised of the OFS 980 fiber. After an additional section of the OFS 980 fiber is spliced to the output C2, the measurement of the relative position between the two-color pulses is performed again. The experimental results show that the 1.56 μm pulse leads the 1.03 μm pulse by an additional 4.1 ps after propagating the 50-cm-long OFS 980 fiber. Thus the total pulse walk-off accumulated in the 3 fiber sections of the shared cavity (WDM3-C1: 22-cm-

#154459 - $15.00 USD Received 12 Sep 2011; revised 2 Nov 2011; accepted 3 Nov 2011; published 15 Nov 2011

long OFS 980 fiber, C1-C2: 112-cm-long HI 1060 fiber, C2-WDM4: 29-cm-long OFS 980 fiber) is estimated to be 6.1 ps, which is larger than the pulse width of the 1.03 μm pulse. This indicates that the 1.56 μm fs pulses pass through a significant portion of the 1.03 μm chirped ps pulse under the passive synchronization process. The measured relative position as well as pulse walk-off is used in the following section to evaluate the influence of the 1.03 μm pulse on the 1.56 μm pulse via the XPM effect.

3. Experimental observation of two-color pulse dynamics

3.1 Dynamics of a single 1.56 μm pulse synchronized to the 1.03 μm pulse

When the pump powers of the two-color mode-locked fiber lasers are kept low, one single 1.56 μm pulse and one single 1.03 μm pulse are generated. For the 1.03 μm pulse, no obvious change in the optical spectrum or autocorrelation trace of the 1.03 μm pulse is observed before and after achieving the passive synchronization. However, for the synchronized 1.56 μm pulse, the variations of the optical spectrum and the location relative to the copropagating 1.03 μm pulse can be clearly observed when the cavity mismatch is detuned. As the cavity length of the mode-locked Yb-fiber laser increases by each step of 2 μm, the center wavelength of the 1.56 μm pulse continuingly shifts towards longer wavelengths, as shown in Fig. 3(a). In the meanwhile, the corresponding relative positions between the two-color pulses measured at the output C1 are shown in Fig. 3(b). These cross-correlation traces show that the 1.56 μm pulse moves toward the leading part of the 1.03 μm pulse as the cavity length of the Yb-fiber laser increased.

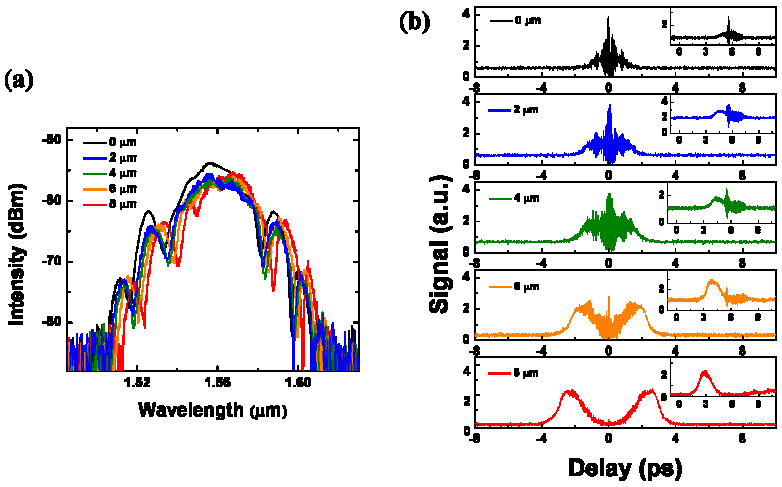

Fig. 3. The optical spectrum of the 1.56 μm pulse (a) and the corresponding relative positions (b) as the the cavity length of the Yb-fiber laser increased. The insets in Fig. 3(b) are the results measured when the Si filter is inserted in the cross-correlator.

The relation among the center wavelength shift, the relative position, and cavity mismatch detuning, provide the more complete evidence to understand the two-color pulse dynamics in our passively synchronized fiber lasers. On the one hand, the 1.03 μm chirped ps pulse is not affected by the 1.56 μm fs pulse, since the pulse width of 1.56 μm pulse is much shorter than that of the 1.03 μm pulse. The net effect from the 1.56 μm pulse is balanced by its leading and trailing parts. On the other hand, 1.56 μm fs pulses pass through a significant portion of the 1.03 μm chirped ps pulse and obtain the required frequency shifts though the XPM effects to maintain the passive synchronization. The influence of the 1.03 μm pulse on the 1.56 μm pulse in the shared fiber sections is evaluated by using the relative position and pulse walk-off as follows. After passing through the 1.03 μm pulse, the 1.56 μm fs pulse can obtain the phase shift via the XPM effect, which can be described as [19]

#154459 - $15.00 USD Received 12 Sep 2011; revised 2 Nov 2011; accepted 3 Nov 2011; published 15 Nov 2011

$$\phi_{XPM} = \sum_{i=1}^{3} \int_0^{L_i} 2\gamma I_0 e^{-\left(\frac{t_i - \Delta_i z}{T_{FWHM}/2\sqrt{\ln 2}}\right)^2} dz, \tag{3}$$

where γ is the Kerr nonlinear parameter of the fiber, I_0 and T_{FWHM} are the peak power and the FWHM pulse width of the 1.03 μm pulse, L_i and Δ_i are the fiber length and the group velocity mismatch in the three fiber sections of the shared cavity, and t_i is the position of 1.56 μm pulse relative to the 1.03 μm pulse at the beginnings of the three fiber sections. Here, for simplicity the pulse shape of 1.03 μm pulse is approximated to be Gaussian and kept unchanged during the copropagation. In Eq. (3) t_{i+1} can be related to t_i by $t_{i+1} = t_i + \Delta_i L_i$ for i = 1,2. In addition, t_1 is replaced by $t_1 = t_{C1} + 3.5$ ps, where t_{C1} is the relative position measured at the output C1 and 3.5 ps is the pulse walk-off between the beginning of the shared cavity and the output C1. Using the actual parameters of the two-color mode-locked fiber lasers, $T_{FWHM} = 2.9$ ps, $L_1 = 0.22$ m, $L_2 = 1.12$ m, $L_3 = 0.29$ m, $\Delta_1 = \Delta_3 = -8.2$ ps/m, and $\Delta_2 = -1.7$ ps/m, the normalized XPM-induced phase shift and its corresponding frequency shift can be evaluated. As shown in Fig. 4 and its inset, both the phase and frequency shifts have been plotted as a function of t_{C1}. This means that our passively synchronized two-color mode-locked fiber lasers can be treated as a 1.5 μm mode-locked Er-fiber laser with an effective intracavity phase modulation that is provided by the copropagating 1.03 μm pulse. In such a case, the position of the 1.5 μm pulse with respect to the effective phase modulation is dependent on the modulation frequency detuning [20]. The passive synchronization should be achieved in the range where the derivative of the frequency shift with respect to the pulse timing is positive, i.e., between –2 ps and 1 ps in the inset of Fig. 4. Thus when the Er-fiber laser has smaller pulse repetition rate than that of the Yb-fiber laser, the 1.5 μm pulse can have the blue shift and move faster in the laser cavity with the net anomalous GVD to achieve the synchronization, or vice versa. The locking range in Fig. 4 is almost in agreement with that observed in Fig. 3(b). Besides, the observation of that the 1.5 μm pulse do not need to be located at the maximum of the phase modulation also indicates the existence of the laser center wavelength restoration effect [1]. The stable passive synchronization is achieved when the effects of the XPM-induced frequency shift and the laser center wavelength restoration are balanced.

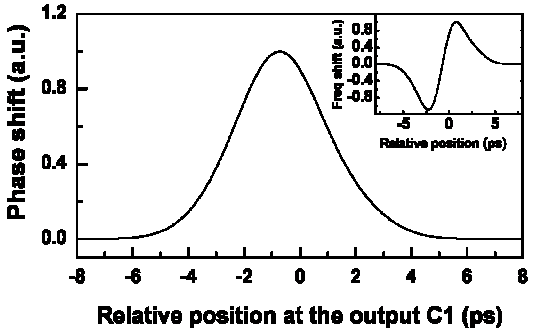

Fig. 4. XPM-induced phase shift and frequency shift (the inset).

3.2 Dynamics of the 1.56 μm bound soliton pair synchronized to a 1.03 μm pulse

When the pump power of the Er-fiber laser is increased while the pump power of the Yb-fiber laser is kept unchanged, the 1.56 μm bound soliton pairs are generated and also can be synchronized with a 1.03 μm pulse [12]. Depending on the cavity mismatch, two different kinds of the 1.56 μm bound soliton pairs, i.e., phase-locked and non-phase-locked, have been both observed. For the synchronized 1.56 μm bound soliton pair with the locked relative

#154459 - $15.00 USD Received 12 Sep 2011; revised 2 Nov 2011; accepted 3 Nov 2011; published 15 Nov 2011

phase, the optical spectrum and the corresponding intensity autocorrelation trace are shown in Fig. 5(a) and 5(b) respectively. In Fig. 5(a), the obvious interferometric visibility and the center peak in the optical spectrum reveal that the relative phase between the bound soliton pair is locked close to zero (in-phase). The period of the modulation on the optical spectrum is 12.5 nm, which is consistent with the close separation of 0.65 ps of the bound soliton pair observed in Fig. 5(b). However, as shown in Fig. 5(d) and 5(e), the bound soliton pair with a wider separation of 2.4 ps does not exhibit any observable modulation, indicating that the relative phase between the bound soliton pair is not locked. In the experiment, the transition between these two different kinds of bound soliton pair is made only by detuning the cavity length mismatch.

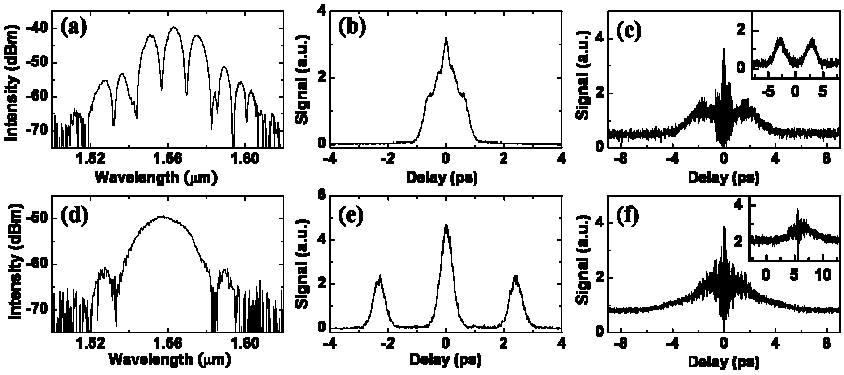

Fig. 5. The optical spectra, autocorrelation traces, and cross-correlation traces of the phase-locked (a)-(c) and non-phase-locked (d)-(f) bound soliton pairs. All the cross-correlation traces are measured at the output C1, except the inset of Fig. 5(c). Only the cross-correlation trace in the inset of Fig. 5(f) is measured using a Si filter inserted in the cross-correlator.

In order to clarify the origin that causes the synchronized 1.56 μm bound soliton pair to exhibit the different characteristics, the locations of these bound soliton pairs relative to the copropagating 1.03 μm pulse in the shared fiber section is also measured experimentally. Figure 5(c) and its inset show the cross-correlation traces measured at the outputs C1 and C2 respectively. The change between the relative positions at the output C1 and C2 shows that the group velocity of the 1.56 bound soliton pair is the same as that of a 1.56 μm single pulse, owing to the same center wavelength of these pulses. The center of the phase-locked bound soliton pair measured at the output C1 is at ~-1.6 ps with respect to the center of the 1.03 μm pulse, which corresponds to the location where the XPM-induced phase modulation (the inset of Fig. 4) is approximately linear. Therefore for the phase-locked bound soliton pair with a very small time separation, the influence of the 1.03 μm pulse can be reasonably approximated by a linear phase modulation. The bound states of soliton in the CGLE with a linear potential has been studied in the theoretical work [15]. The results in Ref [15] show a stable solution of the phase-locked bound soliton pair moving along with the linear potential, which is similar to the observations in our experiment. However, the observed relative phase in our case is close to zero, instead of $\pi/2$. This may be resulted from the fact that the zero phase difference can provides a stronger repulsive force from the effect of larger quintic loss in the CGLE model to avoid the closely bound soliton pair to merge.

When the non-phase-locked bound soliton pair occurs under the passive synchronization, the cross-correlation traces measured at the output C1 without and with suing the Si filter are shown in Fig. 5(f) and its inset respectively. By subtracting the delay of ~5.5 ps introduced by the thin Si filter from the delay time corresponding to the center (i.e., ~6 ps) of the intensity cross-correlation trace in the inset of Fig. 5(f), the center of non-phase-locked bound soliton pair is estimated to be located at ~0.5 ps relative to the center of the 1.03 μm pulse. This indicates the two individual pulses are located at −0.7 ps and 1.7 ps respectively. Therefore the 1.56 μm bound soliton pair experiences an asymmetry influence from the 1.03 μm pulse to

#154459 - $15.00 USD Received 12 Sep 2011; revised 2 Nov 2011; accepted 3 Nov 2011; published 15 Nov 2011

cause the phase unlocked. To our knowledge, the experimental observation of the stable two-pulse bound state with entire loss of observable interference pattern in the optical spectrum was only reported in the Ti-sapphire laser mode-locked by a semiconductor saturable-absorber mirror [21]. One of the possible scenarios underlying the non-phase-locked bound soliton pairs is that the phase difference is dynamically rotating or independently evolving [21, 22]. However, more experimentally dynamical observations of the bound soliton pair's relative phase as well as theoretically numerical investigations based on the CGLE may be needed to further clarify these phenomena.

4. Conclusion

We have carefully measured the relative positions and the walk-off between the two-color pulses along the shared fiber section in passively synchronized mode-locked Er-fiber and Yb-fiber lasers. The influence of a 1.03 μm pulse on the 1.56 μm single pulse as well as bound soliton pairs can be clearly identified as an effective phase modulation from the XPM effect with the walk-off effect taken into account. For the 1.56 μm single pulse under the synchronization, the dependence of the relative position variation and the center wavelength shift on the cavity mismatch detuning is analogous to the typical characteristics of FM mode-locked lasers with the modulation frequency detuning effects. For the 1.56 μm bound soliton pairs under synchronization, two new dynamical behaviors subject to different kinds of relative cross-phase modulation have been observed experimentally. One is the phase-locked soliton pair moving along with the effective linear phase modulation, which are bound very closely and in-phase. The other one, in which two individual pulses are located asymmetrically with respective to the effective phase modulation, exhibits the different dynamical behavior with possibly rotating or independently evolving phase difference.

Acknowledgments

This work is supported by the National Science Council of the R.O.C. under the contracts NSC 99-2112-M-030-002-MY3 and NSC 99-2221-E-009-045-MY3. The authors also gratefully acknowledge the funding from the FJU Physics alumni.

#154459 - $15.00 USD Received 12 Sep 2011; revised 2 Nov 2011; accepted 3 Nov 2011; published 15 Nov 2011